Molecular Crystals and Liquid Crystals

Publication details, including instructions for authors and subscription information:
http://www.tandfonline.com/loi/gmcl20

Synthesis, Characterization and Surface Properties of BPDA-MDA Polyimide

Kyung-Hoe Kim [a], Younghwan Kwon [a] & Yong-Gwon Kim [b]

[a] Department of Chemical Engineering, Daegu University, Kyungbuk, Korea

[b] Korean Fire Protection Association, 35-4 Yovido, Youngdeungpo, Seoul, Korea

Version of record first published: 22 Sep 2010

To cite this article: Kyung-Hoe Kim, Younghwan Kwon & Yong-Gwon Kim (2007): Synthesis, Characterization and Surface Properties of BPDA-MDA Polyimide, Molecular Crystals and Liquid Crystals, 470:1, 145-162

To link to this article: http://dx.doi.org/10.1080/15421400701493646

Mol. Cryst. Liq. Cryst., Vol. 470, pp. 145–162, 2007

ISSN: 1542-1406 print/1563-5287 online
DOI: 10.1080/15421400701493646

Taylor & Francis
Taylor & Francis Group

Synthesis, Characterization and Surface Properties of BPDA-MDA Polyimide

Kyung-Hoe Kim
Younghwan Kwon
Department of Chemical Engineering, Daegu University, Kyungbuk, Korea

Yong-Gwon Kim
Korean Fire Protection Association, 35-4 Yovido, Youngdeungpo, Seoul, Korea

BPDA (3,3′,4,4′-biphenyl tetracarboxylic dianhydride)-MDA (p,p′-methylene dianiline) polyimide was successfully synthesized. Critical surface tension γ_c and surface tension γ_s of BPDA-MDA polyimide film have been estimated by the contact angle method using our quantitative imaging system. The critical surface tensions γ_c were analyzed by a Zisman plot, a Young-Dupré-Good-Girifalco plot, and a log $(1+\cos\theta)$ vs log γ_L plot. The Zisman plot is essentially a downwardly convex curve with polar and hydrogen bonding liquids having $\gamma_c << \gamma_L$. The calculated values of γ_S^d (a dispersion component), γ_S^p (a polar component), γ_S^h (a hydrogen bonding component), and γ_S are 32.13, 4.93, 0.02, and 37.08 $mN \cdot m^{-1}$, respectively.

Keywords: contact angle; critical surface tension; polyimide; quantitative imaging analysis; solid surface tension

INTRODUCTION

Polyimides are widely used in the microelectronics industries as high thermal, chemical, and mechanical resistance layers [1–3]. However, polyimide films are known to absorb water in some amounts, [4–7] despite their relatively high chemical resistance characteristics [8–9]. Water absorbed in polyimide films causes metal corrosion, package

This research was supported by the Daegu University Research Grand, 2005.
Address correspondence to Kyung-Hoe Kim, Department of Chemical Engineering, Daegu University, Kyungsan, Kyungbuk, Korea (ROK), 712-714. E-mail: khk9509@daegu.ac.kr

cracking, delaminating, failures of the adhesion to metal, and degradation of dielectric properties [10–13]. To predict the behavior of polyimides and to optimize their fabrication, it is important to understand the relationship between polyimides structure and their surface properties [14–16]. The surface properties (water sorption and repellency, adhesion) are closely related to the surface tension of polymeric solid. Estimation of surface tension of polymer solid has generally been made by the contact angle method.

The existed experimental techniques for measuring a contact angle are as follows. Several investigators [17,18] simply viewed a sessile drop through a comparator microscope fitted with a goniometer scale, thus measuring the angle directly. Ottewill made use of a captive bubble method [19] wherein a bubble formed by manipulation of a micrometer syringe was made to contact the solid surface. The contact angle might be measured from photographs of the bubble profile, or directly, by means of a goniometer telemicroscope [20]. A reflected light method [21] was engaged in measuring the contact angle. The above-mentioned methods are inaccurate and irreproducible because a testing drop for contact angle measurement can be easily evaporated due to its tiny size and volatility. However, our lab-made quantitative imaging system could provide accurate and reproducible value of a contact angle since the computing system instantly grab the contact angle image and then store it to analyze.

BPDA-MDA polyimide was newly synthesized to investigate the effect of the introduced methylene group on the surface property. A contact angle was measured by a quantitative imaging system to investigate the relationship between a newly synthesized polyimide and its surface property. Three different groups of testing liquids, [22] e.g., dispersion, polar, hydrogen bonding liquids were used to measure the contact angle θ on a BPDA-MDA polyimide film. Critical surface tensions γ_C were evaluated by a Zisman plot, a Young-Dupré-Good-Girifalco plot, and a log $(1+\cos\ \theta)$ *vs* log (γ_L) plot [23]. The surface tension γ_S of BPDA-MDA polyimide was determined by a geometric mean equation and the multiple regression analysis.

1. THEORETICAL BACKGROUND

1.1. Young's Equation

The equilibrium contact angle (abbreviated θ here) for a liquid drop on a solid surface is usually discussed in terms of Young's equation;

$$\gamma_L \cos\theta = \gamma_S - \gamma_{SL} \tag{1}$$

1.2. Critical Surface Tension

1.2.1. Zisman plot. The concept of critical surface tension was first proposed by Fox and Zisman [17,24,25]. An empirical rectilinear relation was found between cos θ and γ_L for a series of testing liquids on a given solid. When homologous liquids are used, a straight line is often obtained. When nonhomologous liquids are used, however, the data are often scattered within a rectilinear band or give a curved line. The intercept of the line at cos $\theta = 1$ is the critical surface tension γ_c.[26] The cos θ *vs* γ_L is known as the Zisman plot.

1.2.2. Young-Dupré-good-girifalco plot. Fowkes, [27] Good, [28,29] Good and Girifalco [30] introduced an interaction parameter Φ_G, defined by.

$$\Phi_G = \frac{W_a}{(W_{c1}W_{c2})^{0.5}} \tag{2}$$

They presented the following equation

$$W_a = \frac{2\Phi_G}{(\gamma_S\gamma_L)^{0.5}} \tag{3}$$

Using Eq.(1) and Young-Dupré's equation

$$W_a = \gamma_L(1 + \cos\theta) \tag{4}$$

Equation (5) can be derived and determine the magnitude of the interfacial tension, γ_{SL}.

$$W_a = \gamma_S + \gamma_L - \gamma_{SL} \tag{5}$$

W_a and γ_{SL} are very important parameters for wettability and adhesion.

Combining Eq.(3) with Eq.(4) leads to the equation of Young-Dupré-Good-Girifalco:

$$1 + \cos\theta = 2\Phi_G\left(\frac{\gamma_s}{\gamma_L}\right)^{0.5} \tag{6}$$

The Young-Dupré-Good-Girifalco plot expressed by the $(1+\cos\theta)$ *vs* $\gamma_L^{-0.5}$ gives rise to a good straight line with the experimental data obtained by the contact angle θ of homologous liquids on a polymer solid. However, in many cases the straight line greatly deviated from the origin with the polarity of liquids [31]. In such cases, the straight line can be expressed as:

$$1 + \cos\theta = \lambda\gamma_L^{-0.5} + \phi \tag{7}$$

where λ and ϕ are the slope and the intercept of $(1+\cos\theta)$ at $\gamma_L^{-0.5}=0$ in the $(1+\cos\theta)$ *vs* $\gamma_L^{-0.5}$ plot known as the Young-Dupré-Good-Girifalco plot. These parameters are constant with homologous liquids. The critical surface tension γ_C can be obtained from the value of γ_L at $\theta\rightarrow 0$.

Using Eq. (7), Young-Dupré's equation (4) and Good-Girifalco's equation (3), and neglecting equilibrium spreading pressure, the Good-Girifalco interaction parameter Φ_G is expressed as:

$$\Phi_G=\left(\frac{1}{2\gamma_S^{0.5}}\right)\left[(2-\phi)\gamma_C^{0.5}+\phi\gamma_L^{0.5}\right] \tag{8}$$

The parameter Φ_G^0, defined as Φ_G at $\theta\rightarrow 0$, is expressed as follows.

$$\Phi_G^0=\left(\frac{\gamma_C}{\gamma_S}\right)^{0.5} \tag{9}$$

1.2.3. The log (1+cosθ) versus log (γ_L) plot. As the interaction between liquid and solid is approximated by the use of the geometric mean law, Φ_0 is defined as the indication of polarity in Φ_G. Furthermore, we also took account of an adjustable parameter X_{LS} within Φ_G as a deviation from the interaction estimated by the geometric law [31]. Thus Φ_G is represented by:

$$\begin{aligned}\Phi_G&=(X_L^dX_S^d)^{0.5}+(X_L^pX_S^p)^{0.5}+X_{LS}\\&=\Phi_0+X_{LS}\end{aligned} \tag{10}$$

Wu [32] reported that the polarity X_j^p was estimated with the solubility parameter δ and the polarity component of the solubility parameter δ^p by the following equation:

$$X_S^p=(\delta^p/\delta)^2 \tag{11}$$

Also, the parameter a, determined with the polarity and X_{LS}, is introduced into Φ_G as follows:

$$\begin{aligned}&\Phi_G=\Phi_0(\gamma_L/\gamma_S)^a\\&a=\left[\log\left(1+\frac{X_{LS}}{\Phi_0}\right)\right]/\log(\gamma_L/\gamma_S)\\&a<0.5\quad\text{for}\quad d\cos\theta/d\gamma_L<0\end{aligned} \tag{12}$$

The Φ_0 is equal to the bonding efficiency parameter of Kaelble and Uy [33]. Therefore, Φ_G^0 is expressed by:

$$\Phi_G^0 = \left[\left(X_C^d X_S^d\right)^{0.5} + \left(X_C^p X_S^p\right)^{0.5}\right](\gamma_C/\gamma_S)^a \tag{13}$$

where X_C^d is the ratio of γ_C obtained with dispersion liquids and γ_C obtained with polar or hydrogen bonding liquids [31]. By solving Eqs. (9) and (13), solid surface tension γ_S can be calculted from Eq. (14):

$$\gamma_S = \gamma_C\left[\left(X_C^d X_S^d\right)^{0.5} + \left(X_C^p X_S^p\right)\right]^{2/(2a-1)} \tag{14}$$

Also, the reversible work of adhesion W_a is expressed by:

$$W_a = 2\Phi_0(\gamma_S^{0.5-a}\gamma_L^{0.5+a}) \tag{15}$$

Consequently, combining Eq. (15) with Young-Dupré's equation (4) leads to:

$$\log(1+\cos\theta) = -\Psi\log(\gamma_L) + \log(2\Phi_0\gamma_S^{0.5-a}) \tag{16}$$

Using Eq. (16), the parameter a is determined with the slope $\Psi = (0.5-a)$ from log $(1+\cos\theta)$ *vs* $\log(\gamma_L)$ plot and γ_C can be found by extrapolating the linear function to $\log(1+\cos\theta) = \log 2$.

1.3. SURFACE TENSION OF POLYMER SOLID

Kitazaki and Hata [22] extended Fowkes' equation [27] to the following equation.

$$\gamma_S = \gamma_S^d + \gamma_S^p + \gamma_S^h \tag{17a}$$

$$\gamma_L = \gamma_L^d + \gamma_L^p + \gamma_L^h \tag{17b}$$

They proposed that the surface tension of polymer film γ_S can be considered as a sum of a dispersion component γ_S^d, a polar component γ_S^p and a hydrogen bonding component γ_S^h. Liquid surface tension γ_L is also expressed as a sum of a dispersion component γ_L^d, a polar component γ_L^p, and a hydrogen bonding component γ_L^h. Using the work of adhesion W_a, the extended Fowkes' Eq. (17) is expressed in the following equation.

$$W_a = 2[(\gamma_L^d\gamma_S^d)^{0.5} + (\gamma_L^p\gamma_L^p)^{0.5} + (\gamma_L^h\gamma_S^h)^{0.5}] \tag{18}$$

By solving the Young-Dupré Eq. (4) and Eq. (18), geometric mean Eq. (19) is obtained.

$$\gamma_L(1+\cos\theta) = 2[(\gamma_L^d\gamma_S^d)^{0.5} + (\gamma_L^p\gamma_L^p)^{0.5} + (\gamma_L^h\gamma_S^h)^{0.5}] \quad (19)$$

Equation (19) can be transformed in Eq. (20)

$$z = (\gamma_S^d)^{1/2} + (\gamma_S^P)^{1/2}x + (\gamma_S^h)^{1/2}y \quad (20)$$

where $x = \sqrt{\frac{\gamma_L^P}{\gamma_L^d}}$, $y = \sqrt{\frac{\gamma_L^h}{\gamma_L^d}}$, $z = \frac{\gamma_L(1+\cos\theta)}{2(\gamma_L^d)^{0.5}}$

The surface tension of polymer solid γ_S and its fractional components $(\gamma_S^d, \gamma_S^p, \gamma_S^h)$ can be determined by contact angles measured by three different group of test liquids [22] and Eq. (20).

2. EXPERIMENTAL

2.1. Synthesis of BPDA-MDA Polyimide

It was investigated how surface properties were affected by introducing methylene group to the main chain of newly synthesized polyimide. Polyimide is an imide group-containing polymer synthesized by condensation polymerization of dianhydride with diamine. Depending on the structure of the chemical radicals attached to the imide group, polyimide can be aliphatic or aromatic, linear or branched.

This study polymerized BPDA (3,3′,4,4′-biphenyltetracarboxylic dianhydride; Chriskev Co., Inc.) with lab-synthesized MDA (p,p′-methylenedianiline). The preparation process of polyamic acid and polyimide of BPDA-MDA demonstrated in Figure 1. A diamine of MDA and a solvent of NMP (*N*-methyl-2-pyrrolidone, Aldrich Chem. Co., Inc.) were introduced into a four-necked flask (500 ml) equipped with a thermocouple, a stirrer, and a nitrogen inlet. The mixtures were stirred thoroughly in a nitrogen environment. After dissolving MDA completely, BPDA was put into the flask at 1:1 stoichiometric ratio. A solvent soluble polyamic acid precusor was formed by the slow reaction of reaction mixtures for 5 h. The solid content of viscous reaction mixtures was about 15% (w/v) by NMP solvent.

A spin coater (Model 301 series, Able Co.) was used to make a thin film from the polyamic acid of BPDA-MDA by coating on silicone wafer. After prebaking the coated film in an 80°C vacuum oven for an hour, an additional process was performed by curing it in 150°C for 30 min, 250°C for 30 min, 350°C for 1 h at 10°C/min of heating rate under nitrogen. A distilled water bath was employed to separate the coated polyimide film from silicone wafer. The separated film was used for contact angle measurement after complete drying in the oven.

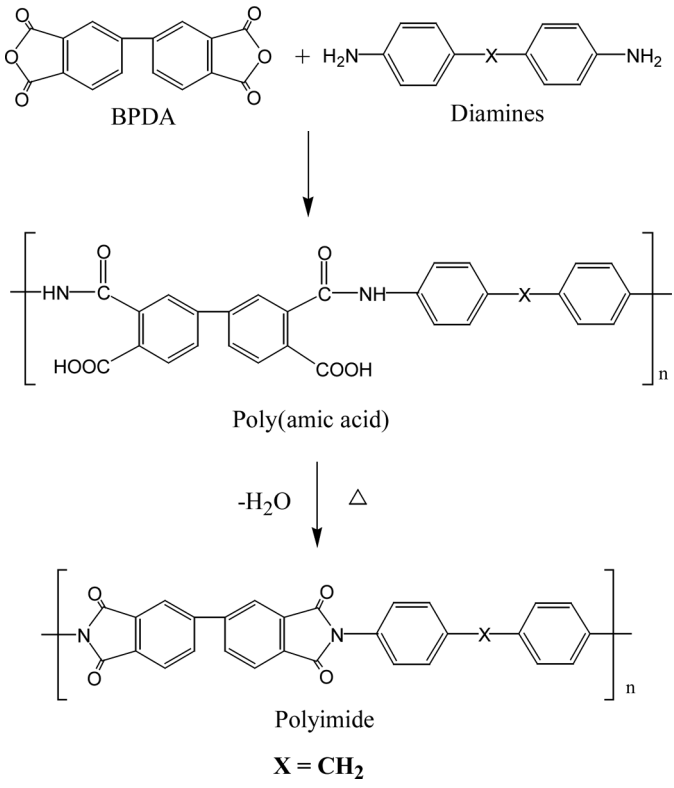

FIGURE 1 Synthetic process of BPDA-MDA polyimide.

2.2. IR Spectroscopy

FT-IR Spectrometer (Genesis II, Mattson Instrument) was used to confirm if a BPDA-MDA polyimide was successfully synthesized. Examining the absorption bands of the carbonyl group (C=O) and the imide ring (C−N) could provide the right information of the imidization reaction.

2.3. Contact Angle Measurement by Quantitative Imaging System

A CCD camera (Model WV-BL 600, Panasonic) was connected to a zoom microscope (Model A52953, Edmund Scientific Ltd.) for acquiring contact angle images by a computer system. A personl computing system saved contact angle images captured by a Frame grabber (Model DT2867, Data Translation Inc.), the CCD camera, and the

zoom microscope. The frame grabber possesses 256 gray scale photography and the resolution of 640×480 pixels. The captured contact angle image was quantitatively analyzed by an imaging software (Global Lab® Image, Data Translation Inc.) and a separate multisync monitor (Syncmaster 1000p, Samsung Co.).

Figure 2 indicates a schematic diagram of the quantitative imaging system. The value of contact angle was determined by the following experimental procedure and imaging analysis method. A microsyringe injected an 1 mm size of a testing liquid to neglect the gravity effect. As soon as a testing liquid in Table 1 was equilibrated, a contact angle image was instantly grabbed. An 1-mm-diameter stainless ball was engaged to calibrate the actual dimension of the enlarged image of the contact angle. Image enhancement was performed to differentiate solid film from the sessile drop and the background from the sessile drop. After determining the radius r of the baseline formed by the solid film and the sessile drop, the height h of the sessile drop was calculated. Since direct reading of the contact angle provided a large experimental error, the contact angle was estimated by the $\theta/2$ method which gave accurate and reproducible results [34,35].

3. RESULTS AND DISCUSSION

3.1. FT-IR Spectra

It is confirmed from Figure 3 that the BPDA-MDA polyimide is successfully synthesized [36]. The srtongest absorption occurs at

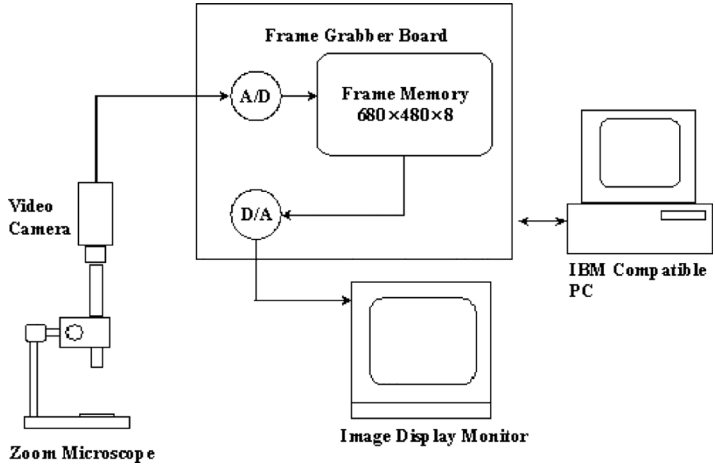

FIGURE 2 Schematic diagram of the image processing system.

TABLE 1 The Contact Angle θ on BPDA-MDA Polyimide Film and Surface Tensions of All Testing Liquids at 20°C [$mN \cdot m^{-1}$]

Species	Liquid	Contact angle θ (°)	γ_L^d	γ_L^p	γ_L^h	γ_L	X_L^p
Dispersion solution	Octane	spreading	21.8	0	0	21.8	0
	Nonane	spreading	22.9	0	0	22.9	0
	Decane	spreading	23.9	0	0	23.9	0
	Undecane	spreading	24.7	0	0	24.7	0
	Tetradecane	spreading	26.7	0	0	26.7	0
	Hexadecane	spreading	27.6	0	0	27.6	0
Polar solution	Hexachlorobutadiene	24.4	35.8	0.2	0	36.0	0.006
	1,2-Dibromoethane	30.8	–	–	–	38.9	–
	α-Bromonaphthalene	32.4	44.4	0.2	0	44.6	0.004
	Tetrabromoethane	43.8	44.3	3.2	0	47.5	0.067
Hydrogen solution	Dipropyleneglycol	38.7	29.4	0	4.5	33.9	0.133
	1,3-Butanediol	55.1	–	–	–	37.8	–
	Polyethyleneglycol	63.5	29.9	0.1	13.5	43.5	0.313
	Diethyleneglycol	62.8	31.7	0	12.7	44.4	0.286
	Ethyleneglycol	70.5	30.1	0	17.8	47.7	0.373
	Water	92.0	29.1	1.3	42.4	72.8	0.600

$1720\,cm^{-1}$ (C=O symmetrical stretching). The more useful bands of imide groups are $1780\,cm^{-1}$ (C=O asymmetrical stretching), $1380\,cm^{-1}$ (C–N stretching), $725\,cm^{-1}$ (C=O bending).

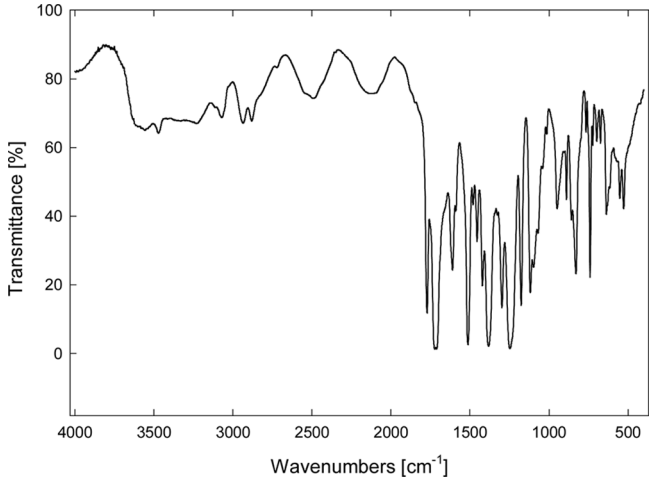

FIGURE 3 FT-IR Spectrum of BPDA-MDA polyimide film.

3.2. Contact Angles

Before measuring the contact angles formed by water on the BPDA-MDA polymide film, a PTFE (polytetrafluoroethylene) film was used to calibrate the quantitative imaging system and its analysis method. The contact angle on the PTFE film is 108 degree, which is corroborated the value in the literature [37–39]. It is verified that the quantitative imaging system and its analysis method can provide accurate and reproducible values of the contact angle. Contact angles were measured by dispersion, polar, and hydrogen bonding liquids in Table 1. Figure 4 is a typical contact angle image of a liquid drop of ethyleneglycol equilibrated on the BPDA-MDA polyimide film. It can be seen from Table1 that the values of the contact angle increases with increasing of the surface tensions of the testing liquids used. The largest contact angle was measured by water whose surface tension is the largest among hydrogen bonding liquids. On the other hand, the smallest contact angle was observed by hexa-chlorobutadiene whose surface tension is the samllest among polar liquids. For a group of dispersion testing liquids, however, contact angles are not observed due to their complete spreading on polyimde film.

3.3. Critical Surface Tensions

The Zisman plots for the BPDA-MDA polymide film are shown in Figure 5. Table 2 displays the critical surface tensions estimated by

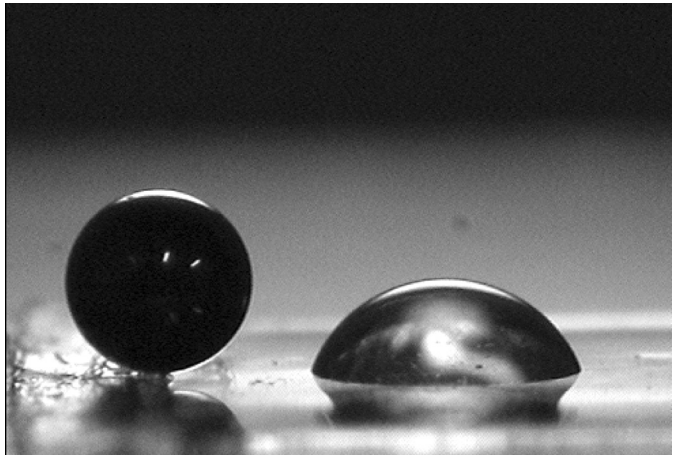

FIGURE 4 Typical contact angle image of a testing liquid drop of ethyleneglycol on BPDA-MDA polyimide film.

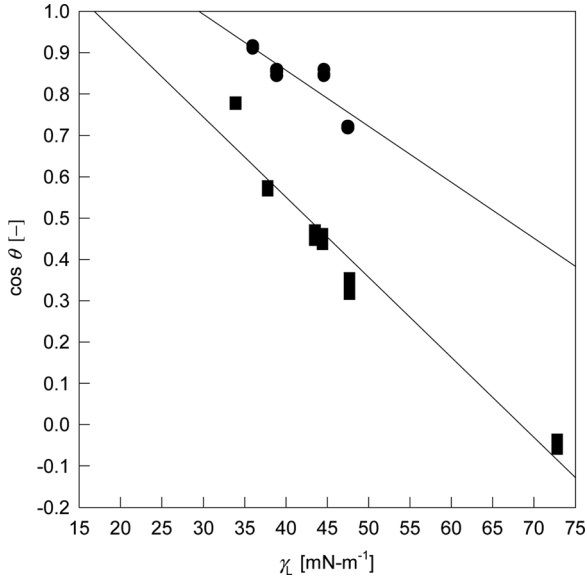

FIGURE 5 Zisman plots for BPDA-MDA polyimide film: •, Polar liquids; ■, Hydrogen bonding liquids.

Figure 5. The values of the critical surface tensions by polar and hydrogen bonding liquids are 29.48 and 16.84 $mN \cdot m^{-1}$, respectively. The critical surface tensions by dispersion liquids can not be obtained because of their complete spreading on the polyimide film. The magnitude of critical surface tension, therefore, increases in the following order: hydrogen liquids < polar liquids. When plotting cos θ as a function of the polarity of different liquids, different values of critical surface tensions γ_C are obtained. The γ_C for polar liquids is 1.75 times larger than γ_C for hydrogen bonding liquids. The larger variation is illustrated as follows.

TABLE 2 The Critical Surface Tensions of BPDA-MDA Polyimide Film and the Constants Determined from the $(1+\cos\theta)$ *versus* $\gamma_L^{-0.5}$ plot

Polyimide	Plot	Testing liquids	γ_c	ϕ
BPDA-MDA	$\cos\theta$ *vs* γ_L	Polar	29.48	
		Hydrogen	16.84	
	$(1+\cos\theta)$ *vs* $\gamma_L^{-0.5}$	Polar	31.29	0.724
		Hydrogen	28.08	– 0.787
	$\log(1+\cos\theta)$ *vs* $\log(\gamma_L)$	Polar	31.20	
		Hydrogen	29.12	

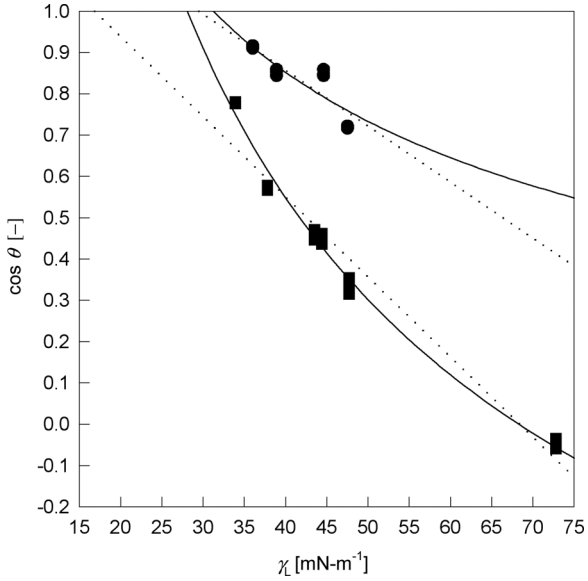

FIGURE 6 Theoretical curves of $\cos\theta$ *vs* γ_L based on Eq. (21) for BPDA-MDA polyimide film: ●, Polar liquids; ■, Hydrogen bonding liquids; — Straight line on the Zisman plots.

On the Zisman plots, empirical relation between $\cos\theta$ and γ_L displays a reasonably straight line when the value of γ_L is in the vicinity of γ_C (in the case of polar liquids). On the other hand, data fitting displays a downwardly convex because a liquid with γ_L much greater than γ_C generally possesses hydrogen bonding [32]. The Zisman plots and the critical surface tensions are corroborated by using the intercept ϕ of $(1+\cos\theta)$ at $\gamma_L^{-0.5} = 0$ from the $(1+\cos\theta)$ *vs* $\gamma_L^{-0.5}$ plot. From Eqs. (6) and (8), the relationship between $\cos\theta$ and γ_L can be rewritten by the following equation.

$$\cos\theta = (2-\phi)\left(\frac{\gamma_C}{\gamma_L}\right)^{0.5} + (\phi - 1) \tag{21}$$

Therefore, Eq. (21) indicates a downwardly convex curve. The γ_C values extrapolated by the Zisman plot and estimated by Eq. (21) are provided as γ_c^E (experimental γ_C) and γ_c^T (theoretical γ_C), respectively. Combining Equation (21) with the ϕ and γ_C values in Table 2 becomes:

$$\text{for Polar liquid} : \cos\theta = 7.138(\gamma_{\mathrm{L}}^{-0.5}) - 0.276$$

$$\text{for Hydrogen bonding liquid} : \cos\theta = 14.768(\gamma_{\mathrm{L}}^{-0.5}) - 1.787$$

Both of the curves fitted by Eq. (21) and the straight dashed line on the Zisman plot by using the least squares method are shown in Figure 6. Better consistency is observed between experimental data and the theoretical curve estimated by Eq. (21). For the polar liquids, γ_{c}^{E} is nearly equal to γ_{c}^{T}. On the other hand, γ_{c}^{E} is obviously smaller than γ_{c}^{T} for the hydrogen bonding liquids. Consequently, it is concluded that the Zisman plot is essentially a downwardly convex curve with polar and hydrogen bonding liquids having $\gamma_{\mathrm{c}} \ll \gamma_{\mathrm{L}}$. This result is consistent with that of Gutowski [40].

Young-Dupré-Good-Girifalco plots represented by the $(1+\cos\theta)$ *vs* $\gamma_{\mathrm{L}}^{-0.5}$ are shown in Figure 7. The straight lines on the $(1+\cos\theta)$ *vs* $\gamma_{\mathrm{L}}^{-0.5}$ fitted by the least squares method greatly deviated from the origin. Table 2 indicates that the values of critical surface tensions by polar and hydrogen bonding liquids are 31.29 and 28.08 $\mathrm{mN \cdot m^{-1}}$, respectively. From the $(1+\cos\theta)$ *vs* $\gamma_{\mathrm{L}}^{-0.5}$ polt, γ_{C} by dispersion liquids also cannot be obtained due to their complete spreading. The magnitude of critical surface tension also increases in the same trend:

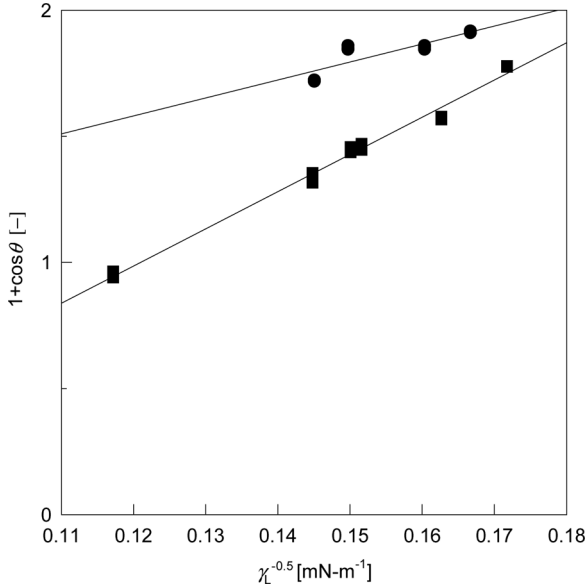

FIGURE 7 Young-Dupré-Good-Girifalco plots for BPDA-MDA polyimide film: ●, Polar liquids; ■, Hydrogen bonding liquids.

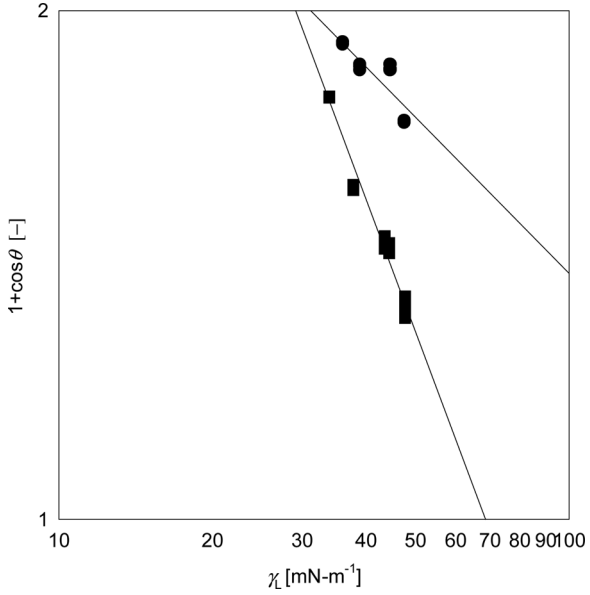

FIGURE 8 Log$(1+\cos\theta)$ *vs* logγ_{L} plots for BPDA-MDA polyimide film: ●, Polar liquids; ■, Hydrogen bonding liquids.

hydrogen liquids < polar liquids. The values of γ_{C} estimated with the $(1+\cos\theta)$ *vs* $\gamma_{\mathrm{L}}^{-0.5}$ polt also have different numbers with varying polarity of liquids used.

The log $(1+\cos\theta)$ *vs* log γ_{L} plots are shown in Figure 8. Experimental data are fitted well with the straight lines fitted by the least squares method. Table 2 indicates that the values of critical surface tensions by polar and hydrogen bonding liquids are 31.2 and $29.12\,\mathrm{mN}\cdot\mathrm{m}^{-1}$, respectively. The order of the magnitude of γ_{C} evaluated with this polt is similar to those on other plots as mentioned before. The γ_{C} values calculated from the log $(1+\cos\theta)$ *vs* log γ_{L} plot also have different numbers with varying polarity of liquids. The γ_{C} values by the Zisman plot are smaller than those estimated by either the Young-Dupré-Good-Girifalco plot or the log $(1+\cos\theta)$ *vs* log γ_{L} plot.

3.4. Solid Surface Tension

Figure 9 represents the best correlation of experimental data using a multiple regression analysis. The surface tension γ_{S} of the BPDA-MDA polymide can be determined by combining contact angles and three known components ($\gamma_{\mathrm{L}}^{\mathrm{d}}$, $\gamma_{\mathrm{L}}^{\mathrm{p}}$, $\gamma_{\mathrm{L}}^{\mathrm{h}}$) with geometric mean Eq. (20). The

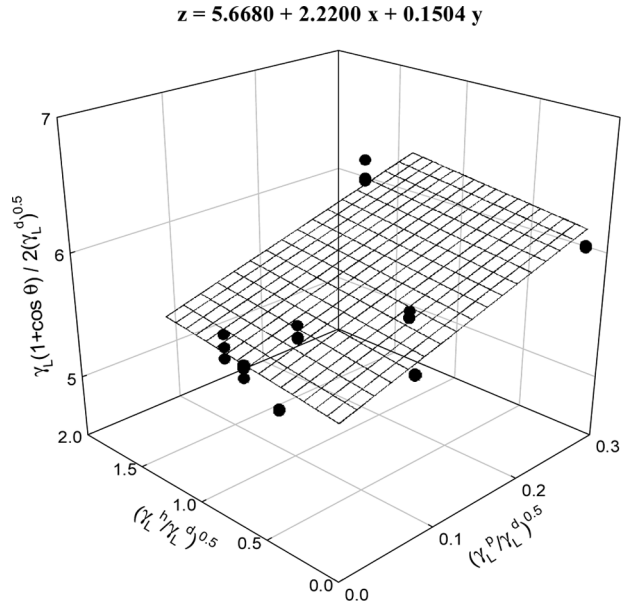

FIGURE 9 Determination of the dispersion (γ_S^d), the polar (γ_S^p), and the hydrogen bonding (γ_S^h) component of the surface tension of BPDA-MDA polyimide by using geometric mean Eq. (20).

calculated values of γ_S^d, γ_S^p, γ_S^h, and γ_S are 32.13, 4.93, 0.02, and 37.08 $mN \cdot m^{-1}$, respectively. Two different Kapton® H films [41] are as follows. The first one is Poly(1,3,5,7-tetraoxo-2,3,6,7-tetrahydro-1H,5H-benzo[1,2-c:4,5-c′]dipyrrol-2,6-diyl-1,4-phenyleneoxy-1,4-phenylene) whose surface tension γ_S is 37.7 $mN \cdot m^{-1}$ and the polarity is 0.223. The second one is Poly(iminocarbonyl-(4,6-dicarboxy-1,3-phenylene)-carbonylimino-1,4-phenyleneoxy-1,4-phenylene) whose surface tension γ_S is 41.1 $mN \cdot m^{-1}$ and polarity is 0.358. The γ_S of BPDA-MDA polyimide is 37.08 $mN \cdot m^{-1}$ which is 0.90 and 0.98 times smaller than those of Kapton® H films, respectively. The polarity of BPDA-MDA polyimide is 0.134 whose value was located between 0.37 and 0.6 magnitudes of Kapton® H films' polarity, respectively.

The value of γ_S^d is larger than γ_L^d of dispersion liquids (21.8–27.6 $mN \cdot m^{-1}$). It can be seen from Table 2 that contact angles are not observed because dispersion liquids completely spread on the polyimide film. The reason of complete spreading is that γ_S^d is larger than γ_L^d. It is not because of both the relation of $\gamma_S > \gamma_L$ and polar properties. The γ_C values in Table 2 are generally smaller than γ_S. The two results are well corroborated with those reported by Kiatazaki and Hata [22].

The γ_S of BPDA-MDA polyimide containing the methylene group only is smaller than that of the polyimide containing both methylene group and the ether group.

CONCLUSIONS

It is confirmed that the BPDA-MDA polyimide is successfully synthesized. Contact angles on BPDA-MDA polyimide film were measured by dispersion, polar, and hydrogen bonding liquids. It can be seen that the values of the contact angle increases with increasing of the surface tension of testing liquids used. For a group of dispersion testing liquids, however, contact angles are not observed due to their complete spreading on the polyimde film. The reason can be illustrated by the relation of $\gamma_S^d > \gamma_L^d$.

The γ_C values by the Zisman plot are smaller than those estimated by either the Young-Dupré-Good-Girifalco plot or the log $(1 + \cos\theta)$ *vs* logγ_L plot. The Zisman plot is essentially a downwardly convex curve with the polar and hydrogen bonding liquids having $\gamma_C < \gamma_L$. Critical surface tensions γ_C calculated from all plots have different values with depending on polarity of liquids. The order of the magnitude of γ_C evaluated with all plots is as follows: hydrogen liquids < polar liquids. The calculated values of γ_S^d, γ_S^p, γ_S^h, and γ_S are 32.13, 4.93, 0.02 and 37.08 $mN \cdot m^{-1}$, respectively. The γ_S of BPDA-MDA polyimide is 37.08 $mN \cdot m^{-1}$ which is 0.90 and 0.98 times smaller than those of Kapton® H films, respectively. The polarity of BPDA-MDA polyimide is 0.134 whose value was located between 0.37 and 0.6 magnitudes of Kapton® H films' polarity, respectively. The γ_S of BPDA-MDA polyimide containing the methylene group only is smaller than that of the polyimide containing both the methylene group and the ether group.

NOMENCLATURE

a: parameter defined in Eq. (12) [—]
h: height of the sessile drop [m]
r: radius of the sessile drop [m]
W_a: work of adhesion [J]
W_c: work of cohesion [J]
X_C^d: ratio of γ_C obtained with dispersion liquid [—]
X_j^d: dispersion fraction of the j component [—]
X_j^p: polar fraction of the j component [—]
X_{LS}: adjustable parameter in Φ_G [—]
X_S^p: the polarity of polymer solid [—]

Greek letters

γ_C: critical surface tension [$mN \cdot m^{-1}$]
γ_c^E: experimental value of critical surface tension [$mN \cdot m^{-1}$]
γ_c^T: theoreticall value of critical surface tension [$mN \cdot m^{-1}$]
γ_L: surface tension of liquid [$mN \cdot m^{-1}$]
γ_L^d: the dispersion component of liquid surface tension [$mN \cdot m^{-1}$]
γ_L^h: hydrogen bonding component of liquid surface tension [$mN \cdot m^{-1}$]
γ_L^p: the polar component of liquid surface tension [$mN \cdot m^{-1}$]
γ_S: surface tension of polymer solid [$mN \cdot m^{-1}$]
γ_s^d: the dispersion component of solid surface tension [$mN \cdot m^{-1}$]
γ_s^h: hydrogen bonding component of solid surface tension [$mN \cdot m^{-1}$]
γ_{SL}: the interfacial tension between the solid and the liquid [$mN \cdot m^{-1}$]
γ_s^p: the polar component of solid surface tension [$mN \cdot m^{-1}$]
δ: solubility parameter [—]
δ^p: polarity component of solubility parameter [—]
θ: contact angle [deg.]
λ: the slope of the Young-Dupré-Good-Girifalco plot [—]
ϕ: the intercept of the Young-Dupré-Good-Girifalco plot [—]
Φ_G: interaction parameter [—]
Φ_G^o: parameter defined in Eq. (9) [—]
Φ_0: indication of polarity in Φ_G [—]
Ψ: slope of the log $(1 + \cos\theta)$ *vs* log γ_L plot [—]

REFERENCES

[1] Sroog, C. E. (1979). *J. of Polym. Sci.: Macromolecular Reviews*, *11*, 161.
[2] Feger, C., Khojasteh, M. M., & Htoo, M. S. (1993). *Advances in Polyimide Science and Technology*, Technomic Publications: Lancaster, PA.
[3] Mittal, K. L. (1984). *Polyimides: Synthesis, Characterization, and Applications*, Plenum Presss: New York, USA.
[4] Wilson, A. M. (1981). *Thin Solid Films*, *83*, 145.
[5] Sacher, E. & Susko. J. R. (1981). *J. Appl. Polymer Science*, *26*, 679.
[6] Wilson, A. M. (1984). Use of polyimides in VLSI fabrication. In: *Polyimides*, 1st ed., Mittal, K. L. (Ed.), Plenum Press: New York, 715–733.
[7] Ree, M., Goldberg, M. J., Czornyj, G., Han, H. S., & Gryte, C. C. (1993). *Polym. Mater. Sci. Eng.*, *68*, 126.
[8] Belluchi, F., Khamis, I., Senturia, S. D., & Lantanison, R. M. (1990). *J. Electrochem. Soc.*, *137*, 1778.
[9] Lee, D. H. (1987). *Polymer(korea)*, *11*, 206.
[10] Sacherand, E. & Sucko, J. R. (1979). *J. Appl. Polym. Sci.*, *23*, 2355.

[11] Denton, D. D., Day, D. R., Priore, D. F., & Senturia, S. D. (1985). *J. of Electronic Materials*, *14*, 119.
[12] Melcher, J., Deben, Y., & Arlt, G. (1989). *IEEE Elecrt. Insul.*, *24*, 31.
[13] Han, H. S. (1993). Ph. D. Thesis, Columbia University: U.S.A.
[14] Merrem, H. J., Klug, R., & Hartner, H. (1989). New developments in photosensitive polyimid. In: *Polyimides*, 2 ed., Mittal, K. L. (Ed.), Plenum Press: New York, 919–931.
[15] Tchangai, E., Segui, Y., & Doukkali, K. (1989). *J. Appl. Polym. Sci.*, *38*, 305.
[16] Jou, J.-H., Huang, R., Huang, P.-T., & Shen, W.-P. (1991). *J. Appl. Polym. Sci.*, *43*, 857.
[17] Fox, H. W. & Zisman, W. A. (1950). *J. Colloid Sci.*, *5*, 514.
[18] Johnson, R. E. & Dettre, R. H. (1965). *J. Colloid Sci.*, *20*, 73.
[19] Gaudin, A. M. (1957). *Flotation*, McGraw-Hill: New York, 163.
[20] Adamson, A. W., Shirley, F. P., & Kunichika, K. T. (1970). *J. Colloid Interface Sci.*, *34*, 461.
[21] Fort, T. & Patterson, H. T. (1963). *J. Colloid Sci.*, *18*, 217.
[22] Kitazaki, Y. & Hata, T. J. (1972). *J. Adhes. Soc. Jpn.*, *8*, 131.
[23] Kano, Y. & Akiyama, S. (1992). *Polymer*, *33*, 1690.
[24] Fox, H. W. & Zisman, W. A. (1952a). *J. Colloid Sci.*, *7*, 109.
[25] Fox, H. W. & Zisman, W. A. (1952b). *J. Colloid Sci.*, *7*, 428.
[26] Zisman, A. (1964). in Treaties on *Contact Angle, Wettability and Adhesion, Advances in Chemistry Series*, No. 43, American Chemical Society: Washington DC, U.S.A., 1–51.
[27] Fowkes, F. M. (1964). in Treaties on *Contact Angle, Wettability and Adhesion, Advances in Chemistry Series*, No. 43, American Chemical Society: Washington DC, U.S.A., 99–111.
[28] Good, R. J. (1964). in Treaties on *Contact Angle, Wettability and Adhesion, Advances in Chemistry Series*, No. 43, American Chemical Society: Washington DC, U.S.A, 74–87.
[29] Good, R. J. (1967). in Treaties on *Adhesion and Adhesive*, Patrick, R. L. (Ed.), Marcel Dekker: New York, U.S.A, Vol. 1, 9–68.
[30] Good, R. J. & Girifalco, L. A. (1960). *J. Phys. Chem.*, *64*, 561.
[31] Kano, Y. & Saito, T. (1988). *Setchaku*, *32*, 396.
[32] Wu, S. (1982a). *Polymer Interface and Adhesion*, Marcel Dekker: New York, 105.
[33] Kaelble, D. H. & Uy, K. C. (1970). *J. Adhes.*, *2*, 51.
[34] Wu, S. (1982b). *Polymer Interface and Adhesion*, Marcel Dekker: New York, 257–259.
[35] Adamson, A. W. (1990a). *Physical Chemistry of Surfaces*, 5th ed., John Wiley & Sons: New York, 389–392.
[36] Ghosh, M. K. & Mittal, K. L. (1996). *Polyimides: Fundamentals and Applications*, Marcel Dekker: New York, 16–18.
[37] Wu, S. (1982c). *Polymer Interface and Adhesion*, Marcel Dekker: New York, 162.
[38] Wu, S. (1982d). *Polymer Interface and Adhesion*, Marcel Dekker: New York, 183.
[39] Adamson, A. W. (1990b). *Physical Chemistry of Surfaces*, 5th ed., John Wiley & Sons: New York, U.S.A., 397–398.
[40] Gutowski, W. (1985). *J. Adhes.*, *19*, 29.
[41] Brandrup, J. & Immergut, E. H. eds. (1989). *Polymer Handbook*, 3rd ed., Wiley-Interscience, John Wiley & Sons: New York, VI/422.